A physical analogue model to analyse interactions between tensile stresses and dissolution in carbonate slopes

Stefano Casini · Salvatore Martino · Marco Petitta · Alberto Prestininzi

Abstract A physical analogue model was developed to analyse the relationship between tensional states in rock masses, seepage and karst processes. Use was made of an experimental apparatus consisting of two hydraulic circuits realized by drilling two holes into each of two blocks of sampled limestone from the central Apennines (Italy). A static load (208.85 kg) was applied to one of the blocks in order to elicit tensile stresses within it. Physical and chemical monitoring data showed that the main process involved was temperature-dependent $CaCO_3$ dissolution. This process was more marked in the loaded block circuit, as Ca^{++} concentration in circulated water reached 54 mg/L, whereas only 28 mg/L was reached in the unloaded one. The interaction between load and dissolution caused the observed opening of microcracks, as confirmed by further increase of water loss and by dilution in the loaded block circuit, resulting in a decrease of Ca^{++} concentration. These findings were confirmed by recording additional water losses after increasing the load up to 445.05 kg. A finite difference numerical model showed that tensile stresses (max 20 kPa) within the loaded block were clustered at the intersection of the main joints with the flowpaths, thus representing points of preferential and accelerated dissolution.

Received: 18 May 2005 / Accepted: 16 May 2006
Published online: 8 August 2006

This study is part of a research project on analogical and numerical modelling for geological risk mitigation being conducted at CERI, Research Centre for Geological Risks of the University of Rome "La Sapienza" (Valmontone, Roma, Italy; http://www.uniroma1.it/ceri; e-mail: ceri@uniroma1.it).

S. Casini
Roma Natura,
Villa Mazzanti, Via Gomenizza 81,
00100 Roma, Italy

S. Martino (✉) · M. Petitta · A. Prestininzi
Dipartimento di Scienze della Terra,
Università degli Studi di Roma (La Sapienza),
P.le Aldo Moro n°5,
00185 Rome, Italy
e-mail: salvatore.martino@uniroma1.it
Tel.: +39-0649914040
Fax: +39-0649914080

Résumé Un modèle analogique a été réalisé pour étudier la relation entre les états de tension dans des blocs rocheux et les processus d'infiltration et de karstification. Un dispositif expérimental, fait de deux circuits hydrauliques réalisés en forant deux trous dans chacun des deux blocs de calcaire prélevés au centre des Apennines (Italie), a été utilisé. Afin de créer des contraintes de tension dans l'un des deux blocs, une charge statique (208.85 kg) lui a été appliquée. D'après les données physique et chimique, le processus impliqué le plus important était la dissolution du calcaire en fonction de la température. Ce processus fut plus important dans le bloc soumis à la charge, avec une concentration en Ca^{++} dans l'eau circulante atteignant 54 mg/L, contre 28 mg/L dans l'autre bloc. L'interaction entre la charge et la dissolution entraîna l'observation de l'ouverture de micro-fissures; le processus a également été confirmé par une perte en eau plus importante et un phénomène de dilution dans le circuit du bloc soumis à la charge, entraînant une diminution de la concentration en Ca^{++}. Ces résultats ont été également confirmés par l'enregistrement de pertes en eau supplémentaires lors de l'augmentation de la charge jusqu'à 445.05 kg. Un modèle numérique aux différences finies a montré que les contraintes de tension (max 20 kPa) au sein du bloc soumis à la charge étaient localisées au niveau de l'intersection entre les joints principaux et les trajectoires d'écoulement, révélant ainsi des zones de dissolution préférentielle et accélérée.

Resumen Se desarrolló un modelo físico análogo para analizar la relación entre estados tensionales en masas rocosas, infiltración, y procesos kársticos. Se utilizó un aparato experimental que consiste en dos circuitos hidráulicos construidos mediante la perforación de dos agujeros en cada uno de los dos bloques de caliza muestreada en los Apeninos centrales (Italia). Se aplicó una carga estática (208.85 kg) a uno de los bloques para generar esfuerzos tensionales dentro de ellos. Los datos de monitoreo físico y químico mostraron que el principal proceso involucrado fue la disolución de $CaC0_3$ dependiente de la temperatura. El proceso fue más intenso en el bloque de circuito cargado donde la concentración de Ca^{++} en agua circulante alcanzó 54 mg/L, mientras que en el bloque sin carga la concentración de Ca^{++} fue solo de 28 mg/L. La interacción entre carga y disolución causó la abertura de microgrietas lo cual fue confirmado por el

 DOI 10.1007/s10040-006-0064-x

incremento posterior de pérdida de agua y por dilución en el circuito de bloque cargado ocasionando un descenso en la concentración de Ca^{++}. Estos resultados fueron confirmados mediante el registro de pérdidas de agua adicionales después de incrementar la carga hasta 445.05 kg. Un modelo numérico de diferencia finita mostró que los esfuerzos tensionales (max 20 kPa) dentro del bloque cargado se aglomeraron en la intersección de las fracturas principales con las trayectorias de flujo representando de este modo puntos de disolución acelerada y preferencial.

Keywords Karst · Fractured rocks · Tensional states · Laboratory experiment · Numerical modeling

Introduction

Various areas of the carbonate central Apennines (Italy), as well as of the carbonate Alps, are affected by deep-seated gravitational slope deformations. These deformations consist of gravity-induced deformational processes acting at large spatio-temporal scale and involving the entire slope. Identifying the interactions between karst aquifer seepage, rock mass stresses, jointing and gravity-induced deformations may be problematic (Martino et al. 2001; Alberto et al. 2004). However, simulating gravity-induced deformation processes through laboratory models (i.e. scale-reduced physical analogue models) and numerical models can help in understanding the evolution of stress-strain features in the rock masses involved. These models can also help substantiate geological–evolutionary models obtained from detailed engineering–geology field data.

The paper deals with gravitational deformations observed in the central Apennines (Mt. Nuria), in the slope area lying close to the San Vittorino Plain (Fig. 1). The slope hosts a major karst aquifer, whose main discharge area encompasses the Peschiera River Springs (mean discharge: roughly 18 m^3/s). Numerous studies (Faccenna et al. 1993; Brunamonte et al. 1994; Nolasco 1998; Capelli et al. 2000; Ciotoli et al. 2001; Salvati and Sasowsky 2002; Petitta et al. 2003: Boni et al. 2004) have been conducted on the karst and karst-associated forms (e.g. sinkholes, dolines, small lakes that fill depressions, reddish soils and caves) occurring in the San Vittorino Plain and nearby mountain slopes. The gravity-induced deformations that affect the investigated slope are closely related to the karst processes: the rock mass spreading induces tensile stresses along subvertical relief bands that represent preferential dissolution zones in the aquifer. It is hypothesized that tensile stresses can induce a significant increase in jointing within the rock mass, due to the opening of new microcracks as well as pre-existing ones, causing an increase in dissolution rate; this effect is also consistent with pre-rupture conditions (Griffith 1920). Consequently, the relief bands (corresponding to scarps or trenches at the surface) often house depressions or sinkholes, whose vertical continuity (up to 100 m) has been demonstrated by recent collapse events (Martino et al. 2004). Construction of a water supply pipeline in the study area made it possible to observe subcircular caves within the slope (up to 15 m wide) in the proximity of the relief bands. The above-reported observations justify, in the analysed case study, the hypothesized linkages among stress-strain conditions of the carbonate rocks affected by gravity-induced deformations, karst aquifer seepage, and water dissolution effects.

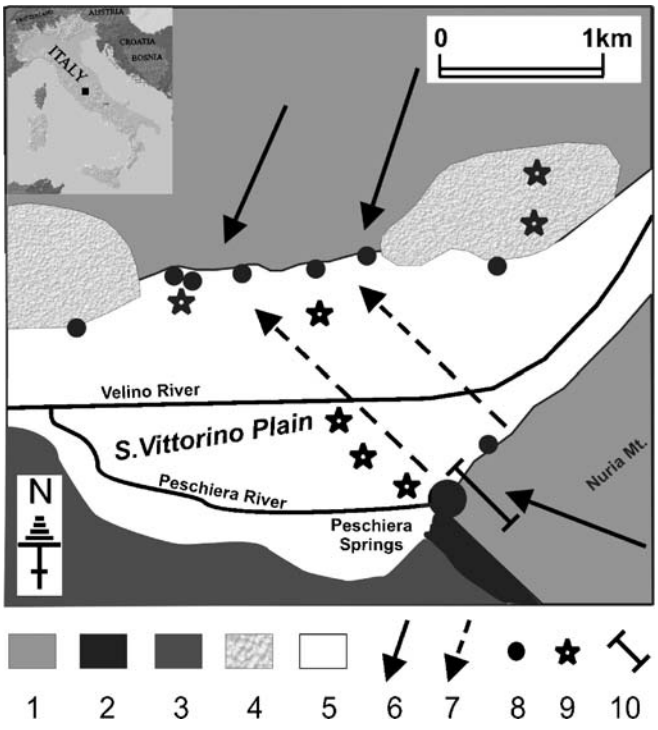

Fig. 1 Hydrogeological sketch of the San Vittorino Plain (central Italy): *1* carbonate aquifer; *2* flysch; *3* alluvial fan facies conglomerates; *4* travertines; *5* alluvial deposits; *6* groundwater flowpaths in carbonate aquifers; *7* groundwater flowpaths through alluvial plain; *8* main springs; *9* sinkholes and lakes; *10* trace of the schematic cross-section of Fig. 3

Many studies have been carried out on the kinetics of calcite dissolution in carbonate aquifers (Plummer and Wigley 1976; Dreybrodt 1981, 1987, 1988, 1997; Groves and Howard 1994). The evolution of their constituent terrains has also been investigated through physical analogue models (Dreybrodt 1991; Novak 1993; Dijk and Berkovitz 1998; Rege and Fogler 1989; Singurindy and Berkowitz 2003), mathematical models (Dreybrodt 1990, 1996; Teusch and Sauter 1991; Bauer et al. 2003), and natural site experiments (Sanford and Konikow 1989; Mylroie and Carew 1995). However, these studies, which were mainly focused on calcite kinetics and karst evolution (Sasowsky and White 1994), have not evaluated in detail the impact of rock mass stresses and strain on dissolution.

 DOI 10.1007/s10040-006-0064-x

As the on-site evidence (Martino et al. 2004) and the numerical modelling (Maffei et al. 2005) both demonstrated the good relationship between landforms and tensile stress conditions for the considered case study, a physical analogue model has been developed in order to analyse the relationship between tensile stresses, seepage and dissolution. Polak et al. (2004) demonstrated that a net reduction in permeability can be induced by an isotropic confining stress applied to an artificial fracture in saturated limestone; nevertheless, the anisotropic stress conditions observed in the gravity-induced lateral spread of the case study area, and replicated by the physical analogue model, are consistent with the opening of microcracks in a tensile-stress field. In particular, this paper discusses the physical analogue model project, the experimental apparatus and the obtained results.

Importance of integrated laboratory and numerical models

The complexity of gravity-induced slope deformations and the spatio-temporal interactions between their forms, evolution and tensional states require an experimental approach to the problems associated with their study. The development of a significant geological-evolutionary model of these gravity-induced phenomena can: (1) help summarize the detailed data collected during geological, geotechnical and site investigations (Martino et al. 2004), and (2) represent the starting point for experimental approaches aimed at validating and refining the data using scale-reduced physical analogue laboratory models, as well as provide support for numerical models (Maffei et al. 2005). In particular, laboratory models of natural phenomena can yield results which can be generalized, if the selected boundary conditions are comparable to those of natural systems. The scientific literature offers plenty of data on simulation of forms and slope-scale processes (Bray and Goodman 1976; Savage and Smith 1986). The use of scale-reduced analogue models (for which downscaling factors should be pre-determined at the design state) can help quantify the investigated phenomena and extrapolate results to similar natural situations (Middleton and Wilcock 1994; Chemenda et al. 2005).

Physical analogue models make it possible to conduct a detailed analysis of the role of different factors in the system, under known (or else controllable) experimental conditions. These models do not necessarily downscale the physical feature being investigated, because they are aimed at analysing it in absolute terms, i.e. they aim to trace the modes of occurrence of the phenomenon and the factors affecting it. Finally, numerical models offer the opportunity to go beyond the technical limits of laboratory models. However, they need numerous and often problematic calibration and fine-tuning. In this respect, the combination of laboratory models with numerical models is essential for refining experimental approaches to the analysis of complex natural phenomena.

Impact of dissolution processes on the Peschiera deep-seated gravitational slope deformations

In the San Vittorino Plain, reports of dolines and small lakes filling karst depressions (Faccenna et al. 1993; Salvati and Sasowsky 2002) are ascribed to the occurrence of deep vertical groundwater conduits. Along its flowpaths, groundwater becomes enriched in components that favour the dissolution of the limestone bedrock of the plain, which is covered by thick alluvium (Ciotoli et al. 2001). These conduits are developing upon major faults, which act as preferential flowpaths for shallow groundwater, and which show surficial evidence of their control on dissolution (lineaments of dolines, depressions and small lakes; Fig. 1).

The investigated slope, located in the south-east portion of the San Vittorino Plain (Fig. 1), has outcrops of Jurassic limestones downslope dipping and strong geomorphological evidence of dislocation by faults. Along the slope, reddish residual soils, resulting from karst dissolution of the outcropping limestone, are frequently found. Of particular significance are large debris cones and slopes, consisting of mostly coarse-grained material, with angular and heterometric clasts, generally well graded longitudinally (Martino et al. 2004). Geomorphological surveys have given additional evidence of gravity-induced slope deformations. Records of deep-seated gravitational deformations in the slope and the occurrence of such forms as sinkholes (Fig. 2) or dolines, downhill of wide scarps or along extensive trenches, infer a close correlation between ongoing gravitational deformations and deep dissolution. The morphological elements observed on the slope and their variety in terms of type and size point to gravity-induced deformations pervading the entire slope system (Martino et al. 2004). The most intense deformations are associated with highly evolved gravitational forms (scarps, trenches and sinkholes), whereas the sectors with more limited deformations show forms that are still in their early stages and with a moderate strain rate (Martino et al. 2004).

The geological-evolutionary model of the slope, is consistent with a sackung deformational process (Zischinsky 1969) which evolves first into lateral spread and then into a rock-block mass deformation (Fig. 3; Martino et al. 2004). Hence, in the initial stages of gravitational processes, the rock mass deformation is governed by primary anisotropies (limestone strata) and by the geometry of relief forms. These forms are associated with subvertical bands where tensile stresses are concentrated. These stresses progressively create tension cracks, actual openings and, ultimately, transversal scarps and longitudinal trenches ("multiple transversal trenches"). The deepening of trenches and scarps is paralleled by the offsetting of loss of material at the surface through the collapse of karst caves, the origin of which is related to the interaction between groundwater dissolution action and tensile stresses concentrated beneath the aquifer, especially near stress-relief bands inside the rock mass (Maffei et al. 2005). Hence, the geological-evolutionary model of the

 DOI 10.1007/s10040-006-0064-x

Fig. 2 Example of a sinkhole on the south-eastern slope of the San Vittorino Plain

slope suggests that unique seepage conditions and tensile stress concentration in the rock mass contribute to the evolution of the observed gravity-induced slope deformations. In actual fact, the calcareous formations that are exposed along the slope have a particular hydrogeological setting which is due to: (1) emergence of the regional aquifer which drains the entire Giano-Nuria-Velino Mts. hydrogeological system, extending for about 1,016 km^2 (Boni et al. 1986, 1995), and (2) presence of facilities for withdrawing groundwater from the Peschiera Springs; these springs, which are partially tapped for water supply purposes, represent the main discharge area of the aquifer.

The amount of dissolved rock per unit of surface area may be estimated, to a first approximation, from the ion content of the Peschiera spring water and by correlating spring discharge and Ca^{++} and Mg^{++} ion concentrations with the aquifer surface area. As is known, the mean discharge of the Peschiera Springs is about 18 m^3/s (Boni et al. 1986, 1995). Analyses of these waters (Table 1) indicated Ca^{++} and Mg^{++} concentrations of 115 mg/L and 15 mg/L, respectively. The recharge area of the Peschiera Springs was determined to be roughly 800 km^2, by dividing the mean discharge of 18 m^3/s by a mean infiltration value of 700 mm/year (Boni et al. 1986). Calcium and magnesium contents proved to be related to dissolution of $CaCO_3$ and $CaMg(CO_3)_2$. Considering the high secondary permeability of the aquifer (facilitated through a dense network of joints, karst caves, sinks and conduits), inducing faster infiltration through the unsaturated zone, both dissolution and precipitation processes were assumed to have negligible effect on the unsaturated zone. Accordingly, the ratio of the atomic weight of the two elements to the molecular weight of calcite and dolomite gave the amount of calcium and magnesium in the aquifer, corresponding to the groundwater outflowing from the Peschiera Springs. Moreover, assuming karst dissolution and related conditions are evenly distributed inside the aquifer, the mass of the carbonates dissolved in the aquifer on a yearly basis (and their weight per unit of

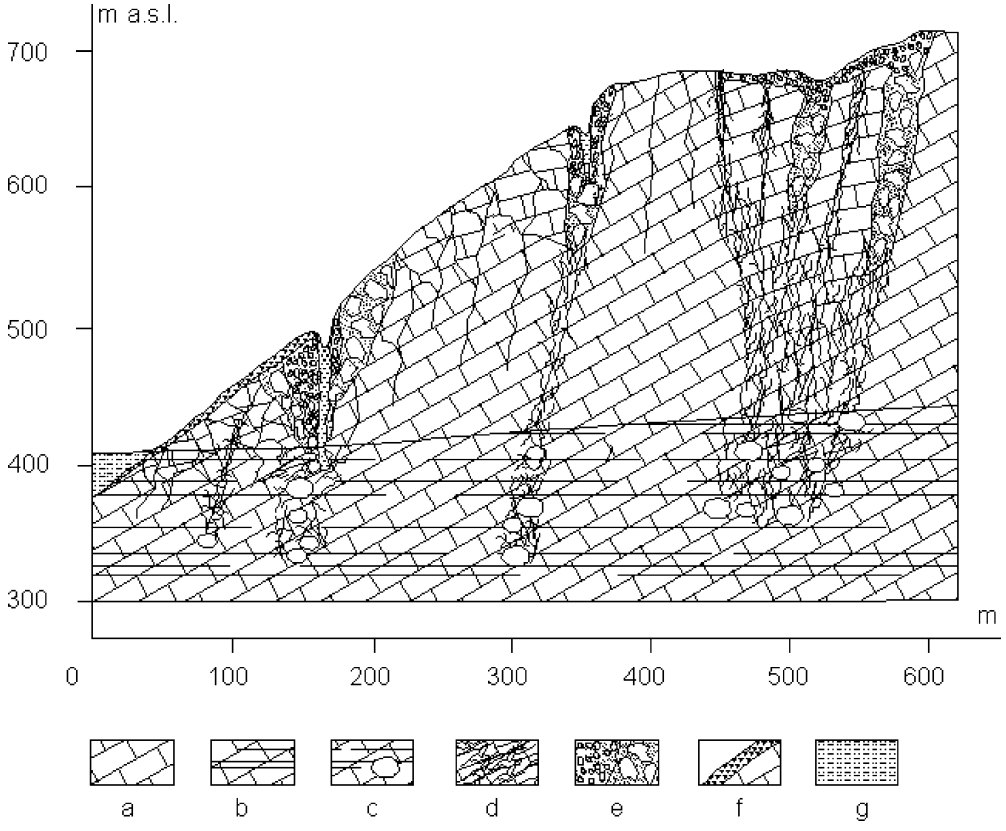

Fig. 3 Schematic cross-section of the investigated slope, see Fig. 1 for location, which exemplifies the relationship between stress-relief bands and karst dissolution, inducing superficial depressions and sinkholes due to the collapse of caves in the aquifer (modified from Martino et al. 2004; Maffei et al. 2005). Keys of the legend: *a* unsaturated limestone, *b* limestone aquifer, *c* caves in the aquifer, *d* highly jointed limestone, *e* debris filling trenches and depressions, *f* slope debris, *g* alluvia

 DOI 10.1007/s10040-006-0064-x

Table 1 Chemical composition of the Peschiera Spring water (Eco Consulting Ambiente Srl, 1993, personal communication)

Chemical composition of Peschiera Spring water	
Temperature	11.00°C
pH	7.20
Conductivity at 20°C	577.00 (μS/cm)
Residuum at 180°C	410.00 (mg/L)
Ammonium	0.00 (mg/L)
Nitrite	0.00 (mg/L)
Nitrate	2.35 (mg/L)
Chloride	3.80 (mg/L)
Sulphate	9.90 (mg/L)
Calcium	115.00 (mg/L)
Magnesium	15.00 (mg/L)
Iron	0.00 (mg/L)
Sodium	2.50 (mg/L)
Potassium	2.00 (mg/L)
Carbon dioxide	25.00 (mg/L)
Bicarbonate	415.00 (mg/L)
Sulphured hydrogen	0.00 (mg/L)

total aquifer surface area) was calculated (Table 2). Taking into account the mean discharge of the Peschiera Springs (18 m^3/s), the dissolved carbonates were calculated to be 5.27×10^5 kg/day, i.e. about 2.40×10^5 kg $year^{-1}$ km^{-2}. Supposing the mean density of carbonate rocks in the study area is 2,700 kg/m^3, the volume of dissolved rock per year km^{-2} was calculated to be about 89 m^3, corresponding to a sphere with a diameter of roughly 5.5 m.

To get additional information on the role that such physical processes might play in the evolution of the investigated deformations, a physical analogue model was built. The model was targeted to analyse the relationship between tensile stress concentration, seepage and karst dissolution, taking into account the key features of the natural slope. Simplification of the model was required both to facilitate data collection and processing, and to minimize the number of uncertain parameters, while the boundary conditions were also monitored.

Design of the physical analogue model

The geological and hydrological elements observed in the natural system and considered in the reference geological-evolutionary model were transposed into the physical analogue model. This was a key stage in the design and construction of the laboratory model. In particular, the model took into account that most of the limestone outcrops had secondary permeability. Furthermore, the model was intended to simulate the tensile stresses that, in the natural system, were concentrated beneath the aquifer (Maffei et al. 2005). These features were replicated in the physical analogue model as follows:

- The limestones of the natural slope were represented by samples taken from the outcrop, characterized by a dense network of joints and microcracks.
- Canals and conduits were replicated by boring two holes into the sagittal plane of squared samples, so as to induce a non-laminar flow.
- The concentration of tensile stresses beneath the aquifer was simulated by subjecting the limestone to a load acting on one of the faces of the squared block, in order to produce tensile stresses normally oriented with respect to the plane in which the seepage holes are located; the simulated stress-strain conditions were similar to those induced in a standard Brazilian test, using cylindrical specimens of rock (Wittke 1990). The resulting tensile stresses were not intended to cause failure conditions in the blocks (such as rupture cracks), but to induce extensional deformations giving rise to microcracks.

The physical analogue model was based on an experimental apparatus consisting of two similar systems. Each system had a hydraulic circuit passing through a block of limestone collected from the slope. The two systems were separate and independent, but placed side by side so as to provide similar boundary conditions (Fig. 4). Prior to testing, the two limestone blocks were squared to a size of 30×35×18.5 cm and their measured weights were 51.67 and 51.50 kg, respectively, corresponding to very similar density values. Additionally, the mapping of the joints observed on the surfaces of the two blocks made no significant difference in the joint frequency, number and persistence. Two diagonal rectilinear holes (diameter = 8 mm) were bored into each block; the holes were parallel to the greatest dimension of the block and inclined by about 15° with respect to its horizontal plane (Fig. 4a).

An experimental study on the kinetics of natural mineral waters (Defrancesco et al. 1997) gave useful inputs to the design of the hydraulic circuits used in the experimental apparatus for the physical model. Reference was also made to the results of an experimental study recently reported by Singurindy and Berkowitz (2003). These authors tested a system for simulating hydraulic circulation through limestone samples in order to investigate carbonate dissolution and consequent changes in hydraulic conductivity versus acid meteoric precipitation. In the experimental apparatus used in this study, the circuit that fed recirculating water to each block consisted of opaque plastic tubes and tanks. This circuit induced a non-laminar flow at the intersection between the two diagonal holes. In particular, the first glass container served as the lower collection tank, which housed two electrically

Table 2 Calculation of calcite and dolomite contribution from the aquifer to Ca^{++} and Mg^{++} in the Peschiera groundwater

Carbonates	Mass (mg/L)
Ca^{++}	115.00
Mg^{++}	15.00
$CaMg(CO_3)_2$	113.73
$Ca^{++}{}_{dolomite}$	24.72
$Ca^{++}{}_{calcite}$	90.28
$CaCO_3$	225.43

 DOI 10.1007/s10040-006-0064-x

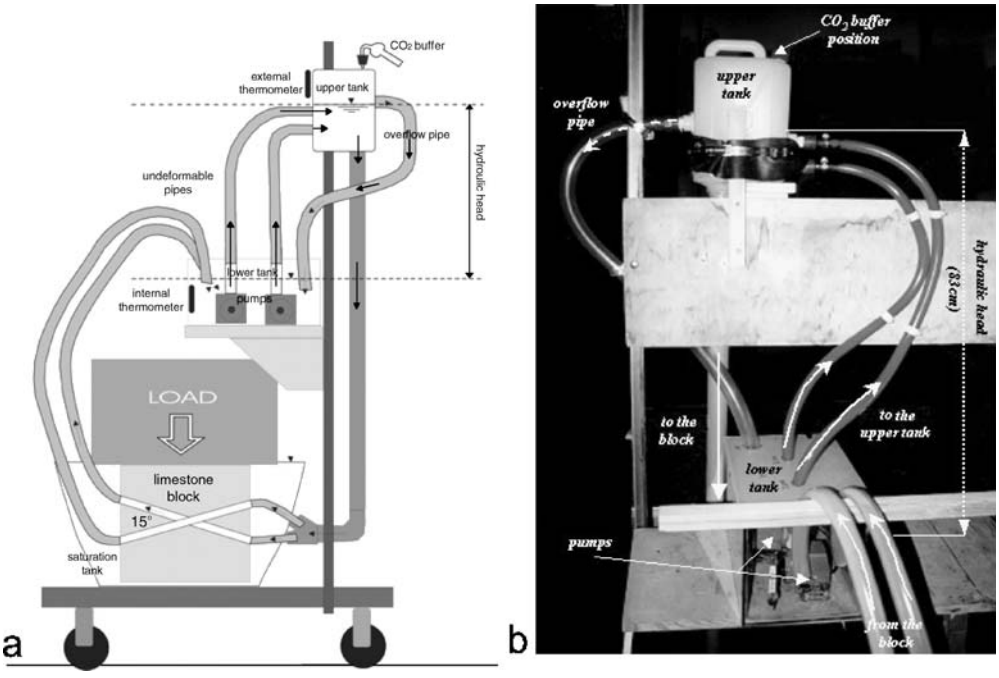

Fig. 4 **a** Design of the physical analogue laboratory model (*loaded block*). The unloaded block circuit had the same design, except without the load. **b** Detailed view of the realized circuit for one of the blocks

driven pumps (steady-state flow rate: 8 L/min). The tank was placed downstream of the block and had an outer black cardboard coating which screened light radiation and minimized the growth of algae and microorganisms. A 3-L polyethylene tank was used for the upper tank, from which the water was pumped and fed by gravity into the holes of the block, thus closing the hydraulic circuit. A chemical buffer system was inserted onto the opening of the upper tank. The buffer system consisted of a calcium chloride tube with NaOH pellets and $CaCl_2$ powder, separated by layers of cotton wool. Its function was to stabilize the partial pressure of carbon dioxide (pCO_2) and minimize water evaporation (Pocar 1996). The water level difference between the upper tank and the lower tank represented the total hydraulic head loss (roughly 80 cm), which occurred during passage of water through the limestone blocks and the tubes and fittings of the apparatus. The circuit was designed to lose most of the hydraulic head through the diagonal holes in each limestone block. Both blocks were housed in PVC tanks with a capacity of over 100 L, filled with distilled water to which 1% H_2O_2 was added. In the design of the experimental apparatus, these tanks had the purpose of keeping the two rock masses saturated and to add thermal mass, i.e. to dampen external temperature excursions. Before the experiment, each hydraulic system was tested for 2 weeks and washed with distilled water. At the beginning of the experiment, both circuits inside the limestone blocks were filled with 10 L of distilled water, to which 1% H_2O_2 was added in order to sterilize the solution.

During the experiment, one of the two blocks was subjected to a static load in order to elicit tensile stresses inside it. The load was applied by means of a column of lead plates with a total mass of 208.85 kg. Subsequently, the static load was increased by 236.20 kg by the addition of lead plates, reaching a total mass of 445.05 kg. The experimental apparatus operated from 14 June 2001 to 12 March 2002 (273 days), continuously feeding water to the two blocks. (The experimental apparatus was occasionally out of service owing to power failures or to its transfer to other rooms and, in August 2001, the experiment was interrupted for about 2 weeks owing to the summer closure of the laboratories.) The physical parameters of the apparatus (ambient temperature, circulating water temperature, hydraulic conductivity and water level in the lower tank) were monitored at intervals of a few hours on the first day of operation and subsequently on a daily basis. The monitoring frequency was progressively reduced as the experiment advanced. At longer intervals, water samples were collected from the circuits of the two rock masses. The water was analysed via atomic absorption spectrophotometry (ICP Varian Vista RL, CCD simultaneous ICP-AES) in order to determine its Ca^{++}, Mg^{++}, Na^{+} and K^{+} contents. The same method was used for analysing a solution obtained with dissolved limestone powder, which showed concentrations of Ca^{++} and Mg^{++} of 98 and 0.47%, respectively, and which represent the main components of the analysed rock. The water sampled and lost by evaporation as well as through the opened cracks was always replaced with the same volume of distilled water. Since experimental conditions and mode of sampling were the same for the two blocks, observed differences in water loss were mainly attributed to leakage from opened cracks. After the first week, the measured water losses were higher in the loaded block circuit

 DOI 10.1007/s10040-006-0064-x

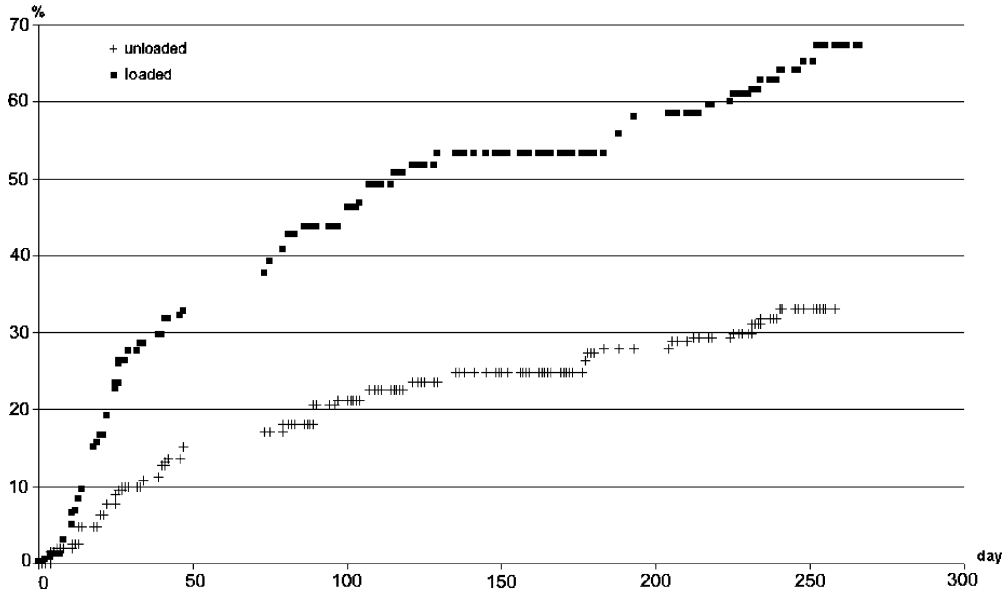

Fig. 5 Percentage of cumulative water loss (replaced with distilled water) during the experiment on daily basis

(Fig. 5). Furthermore, 1% H_2O_2 was added every 15 days in order to ensure biologically sterile conditions to the aqueous solutions flowing in the circuits.

Experimental results

Throughout the experiment, the temperature of the water circulating inside the blocks was, on average, about 3°C above external temperature (Fig. 6a). The measured temperatures showed an increasing trend from day 1 to day 76; subsequently a major decreasing trend was observed until day 171, related to seasonal variations. The effect of temperature on carbonate dissolution has been reported in many studies (Alkattan et al. 1998; Liu and Dreybrodt 1997; Lennart Sjoberg and Richard 1984; Plummer et al. 1978). During the experiment, temperature was monitored but not forced. As the blocks were subjected to the same temperature variations, different dissolution rates were supposed to depend on the additional load. During the experiment, hydraulic head variations in the two circuits stayed below 1 cm; as these variations corresponded to about 1% of the total hydraulic head, their effects on the dissolution process were to be assumed negligible (Fig. 6b).

The electrical conductivity measured in the hydraulic circuits of the rock masses (Fig. 7) by a WTW LF330 conductivity meter showed a sharp upward trend in the first 2 weeks corresponding to the stabilization stage. In this period, the electrical conductivity measured in the loaded block circuit was constantly and significantly higher than the one of the unloaded block circuit. Subsequently, the electrical conductivity of the two circuits tended to converge to 185–195 μS/cm. Starting from day 171, microcracks presumably opened in the loaded block limestone, creating an intercommunication between the internal circuit and the water of the saturation tank and thus reducing the electrical conductivity to minimum values of 165–175 μS/cm in the internal circuit and concurrently increasing the water loss rate. Starting from day 232, the electrical conductivity of the solution inside the loaded block sharply dropped to a minimum of about 159 μS/cm, owing to the increase of the load from 208.85 kg to 445.05 kg. The dilution of the solution was attributed to the further opening of the microcracks existing in the limestone and/or to newly formed microcracks. Conversely, in the same period, the conductivity of water in the unloaded block circuit continued to rise until reaching values of approximately 200 μS/cm (Fig. 7).

Based on physically measured values, five experimental stages were distinguished: (1) initial stabilization stage (14 days) when dissolution rate was higher in the loaded circuit; (2) steady-state stage (day 15–76); (3) temperature-induced dissolution stage (day 77–171) when dissolution in both circuits significantly increased (about 25%) while temperature had a seasonal decrease (by about 13°C); (4) microcracks-induced dilution stage (day 172–231), only for the loaded block circuit; (5) overload-induced dilution stage (day 232–273), only for the loaded block circuit.

Ca^{++} and Mg^{++} concentrations, measured in the aqueous solutions of the two circuits inside the blocks, were the calculated net of dilutions due to systematic addition of distilled water and normalized to a volume of 10 L. These values clearly showed an upward trend in the first 6 months of operation of the experimental apparatus and then tended to stabilize. In particular, Ca^{++} stabilized at around 54 mg/L in the loaded block and around 28 mg/L in the unloaded one, whereas Mg^{++} stabilized at around 0.47 and 0.31 mg/L, respectively. Additionally, during the stabilization stage, the concentrations of both ions remained higher in the loaded block circuit (Fig. 8). Starting from day 172, as expected from electrical

 DOI 10.1007/s10040-006-0064-x

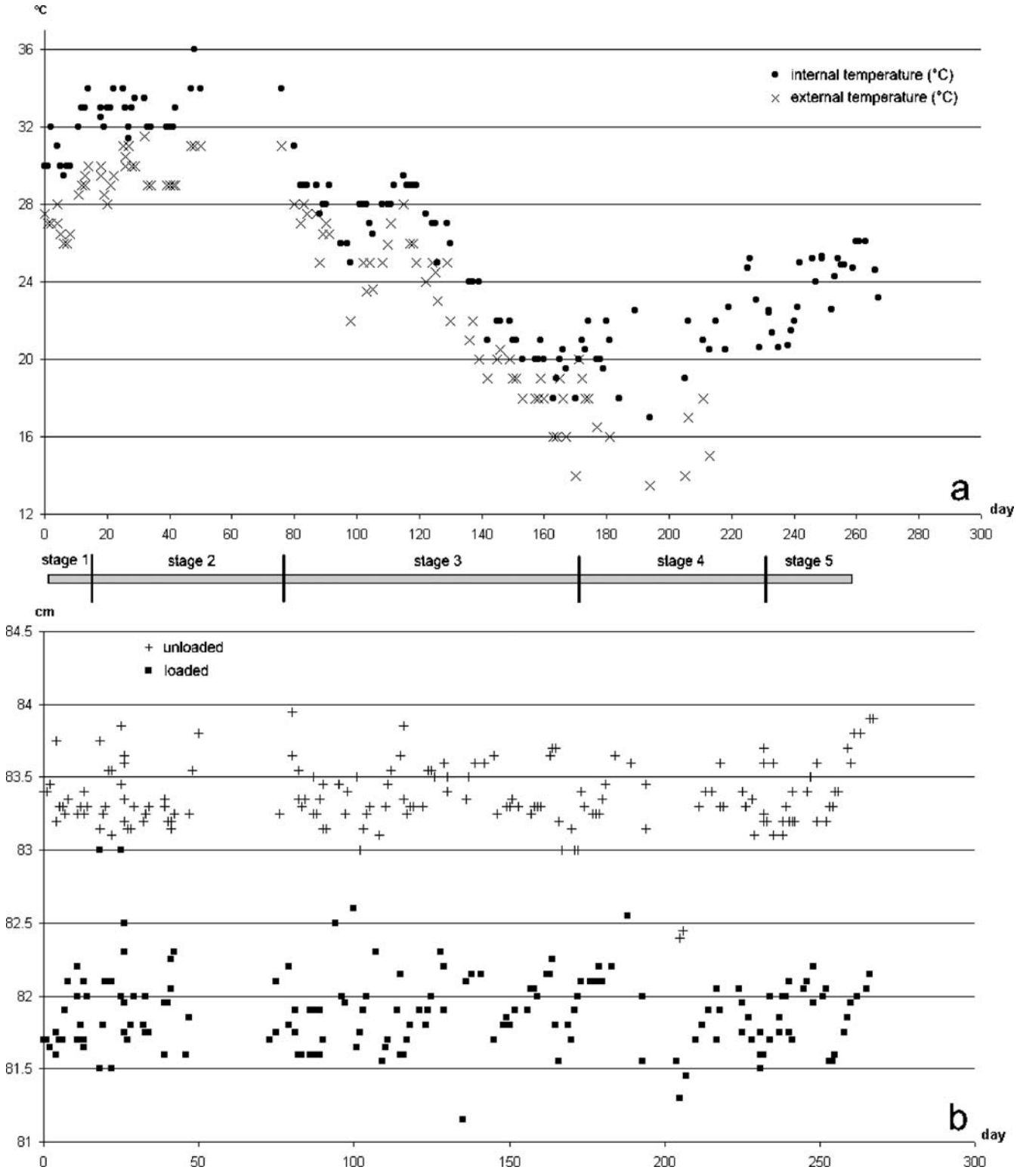

Fig. 6 **a** Temperature for both systems and **b** hydraulic head measured during the experiment

conductivity values, both Ca^{++} and Mg^{++} concentrations dropped to about 48 and 0.34 mg/L in the loaded block circuit, respectively. A lower concentration was recorded after increasing the load (day 232), which caused Ca^{++} and Mg^{++} to fall further to about 44 and 0.12 mg/L, respectively. In reference to a pH_{max}=7.2, a temperature T_{min}=16°C and the highest measured concentrations of Na^{+} (54.29 mg/L), K^{+} (0.92 mg/L), Ca^{++} (78.77 mg/L) and Mg^{++} (0.46 mg/L), the concentration of HCO_3^{-} and the calcite saturation index, computed by the use of SOLMINEQ88 code (Kharaka et al. 1988), demonstrated that, during the experiment, the Ca^{++} precipitation process

 DOI 10.1007/s10040-006-0064-x

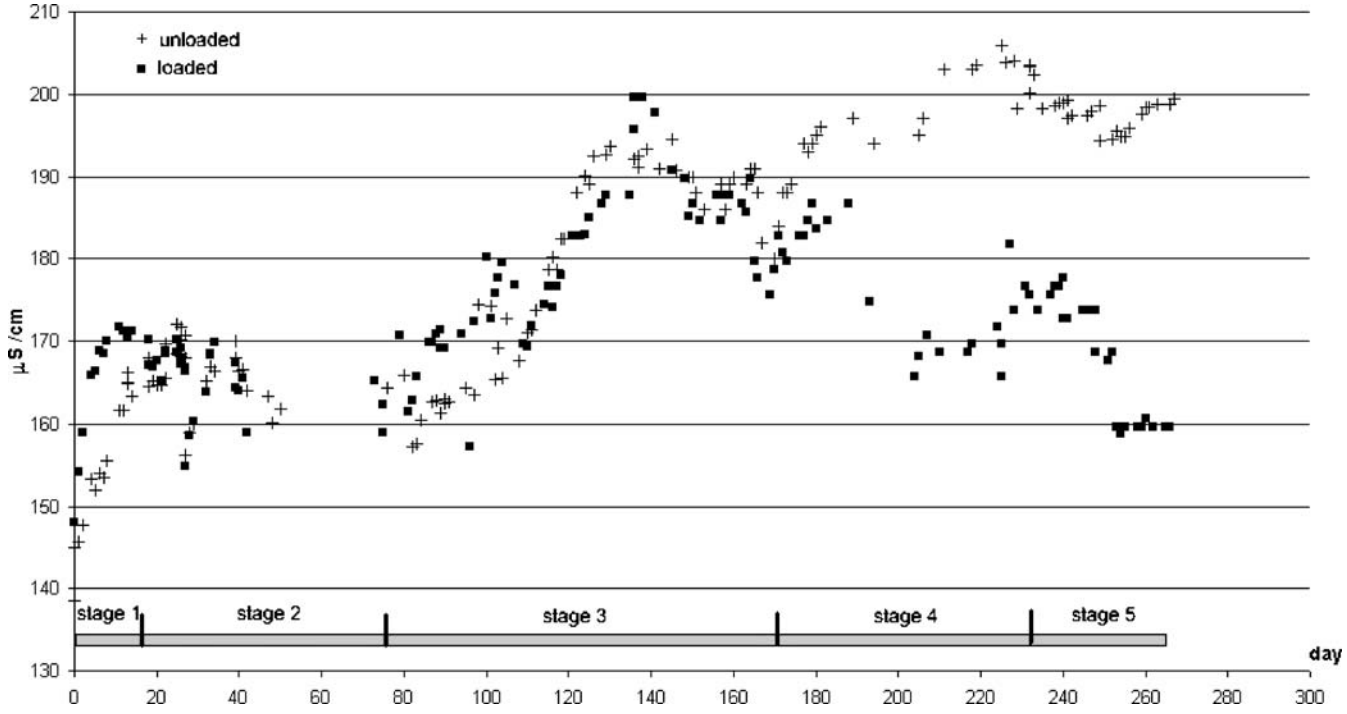

Fig. 7 Electrical conductivity measured during the experiment and normalized to 25°C

did not occur, because the saturation threshold was never reached.

The correlation between electrical conductivity and Ca^{++} and Mg^{++} content is shown in Fig. 9. The limestone dissolution process mainly involved these two cations. A strong correlation with Ca^{++} was found (Fig. 9a). A first group of data pertaining to the unloaded block circuit and to the loaded block circuit represented the two initial stages. From the third stage, data from the unloaded block circuit showed the same trend with increasing Ca^{++} concentrations. Another parallel trend with higher Ca^{++} content, corresponding to the loaded block circuit, was observed in the last three stages. These findings were consistent with: (1) the constant dissolution rate during the temperature-induced dissolution stage (No. 3), for the two circuits and (2) the stopping of dissolution due to dilution during the last two stages (Nos. 4 and 5), only in the loaded block circuit after microcracks opening. The low content of Mg^{++} did not reveal a direct correlation with electrical conductivity values (Fig. 9b). Conversely, after the first 2 weeks (stabilization stage), Na^{+} and K^{+} remained steady at around 30 and 1 mg/L, respectively, in both circuits; this finding was consistent with the fact that Na^{+} and K^{+} contents in the two solutions could not be attributed to limestone dissolution processes.

Experimental measures were consistent with the following findings:

- A good correlation was observed between temperature and electrical conductivity, as the higher temperature values corresponded to the lowest electrical conductivities measured
- The Ca^{++} precipitation process did not occur
- The decreasing concentration of solutes in the water in the circuits (correlated with increasing water losses from the blocks toward the saturation tanks), was consistent with opening of microcracks in the loaded block.

The statistical observation of Ca^{++} concentration values grouped in the five stages highlighted the differences between the unloaded and loaded block circuits (Fig. 10): the unloaded block circuit showed an increasing trend with well grouped values (low standard deviation), whereas the loaded block circuit showed a rapid increase of the Ca^{++} content with high dispersion of the values. At the same time, the five identified stages were well defined: in the unloaded block circuit the initial and final stages showed constant values. In the loaded block circuit, the two final stages showed the decrease of the Ca^{++} concentration due to the dilution effect caused by microcrack opening (stage 4) and by the overload applied during stage 5.

The data obtained from physical and geochemical monitoring of the physical analogue model and described so far, demonstrate greater dissolution in the loaded block circuit, whose static overload elicits tensile stresses. Under these experimental conditions, the opening of microcracks in the limestone establishes intercommunication between external saturation water and block circuit water, thereby diluting the concentration of dissolved salts in the latter. These microcracks are associated with overload and elicited tensile stresses. Moreover, the above results are substantiated by the following common boundary conditions: (1) the measured density of the two blocks as well

 DOI 10.1007/s10040-006-0064-x

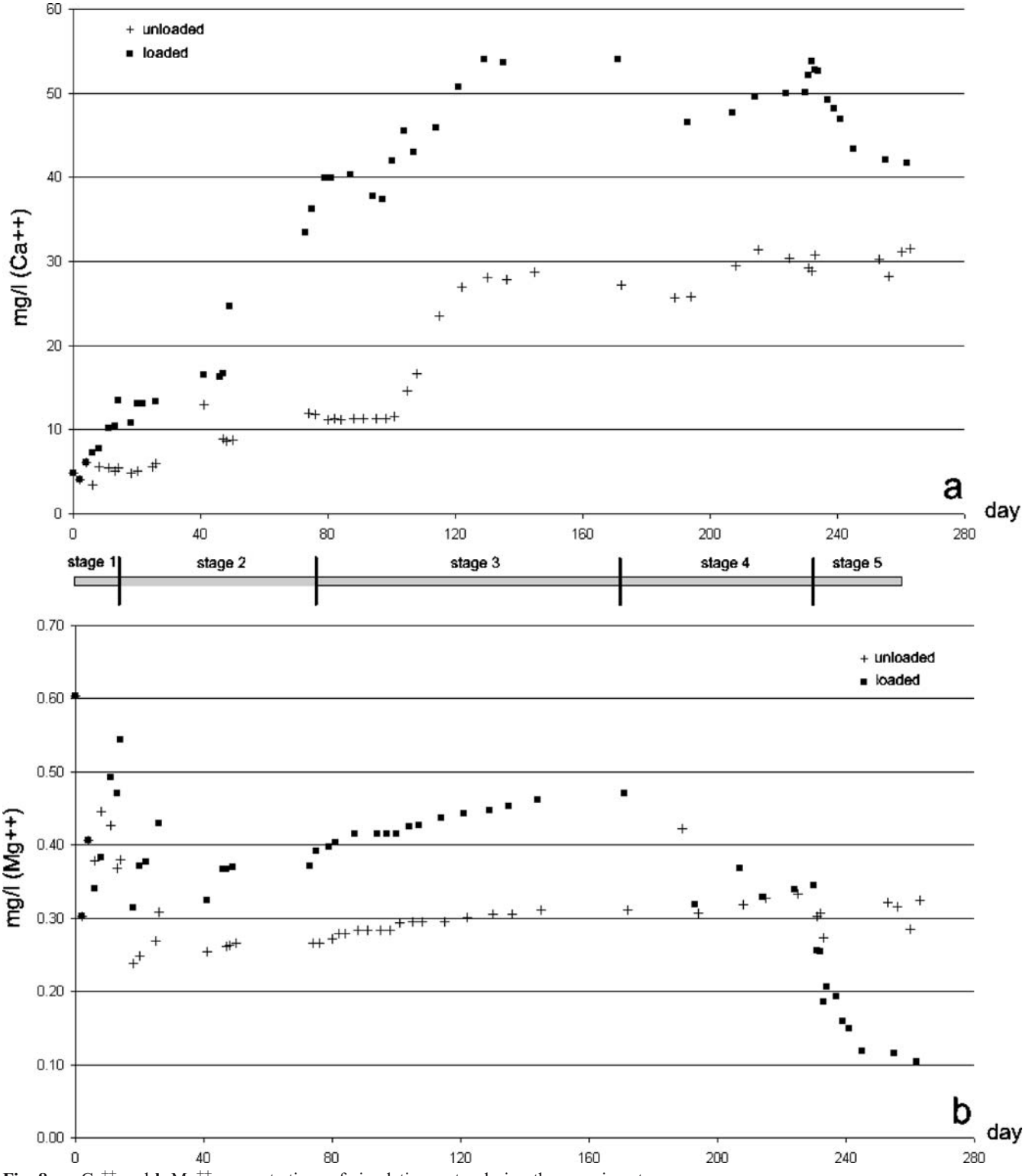

Fig. 8 **a** Ca^{++} and **b** Mg^{++} concentrations of circulation water during the experiment

as the number of joints, mapped before the experiment on their surfaces, were strictly comparable; (2) the loaded block circuit showed smaller hydraulic head; for instrumental reasons, this load remained about 2 cm smaller than that of the unloaded block circuit, (3) the two rock masses had similar initial and boundary flow conditions and (4) the volume of circulating water and use of distilled water for initial solution were identical. All these findings are consistent with the assumption underlying the geological-evolutionary model of the slope, i.e. an interaction between tensional states and dissolution effects of karst aquifer seepage.

 DOI 10.1007/s10040-006-0064-x

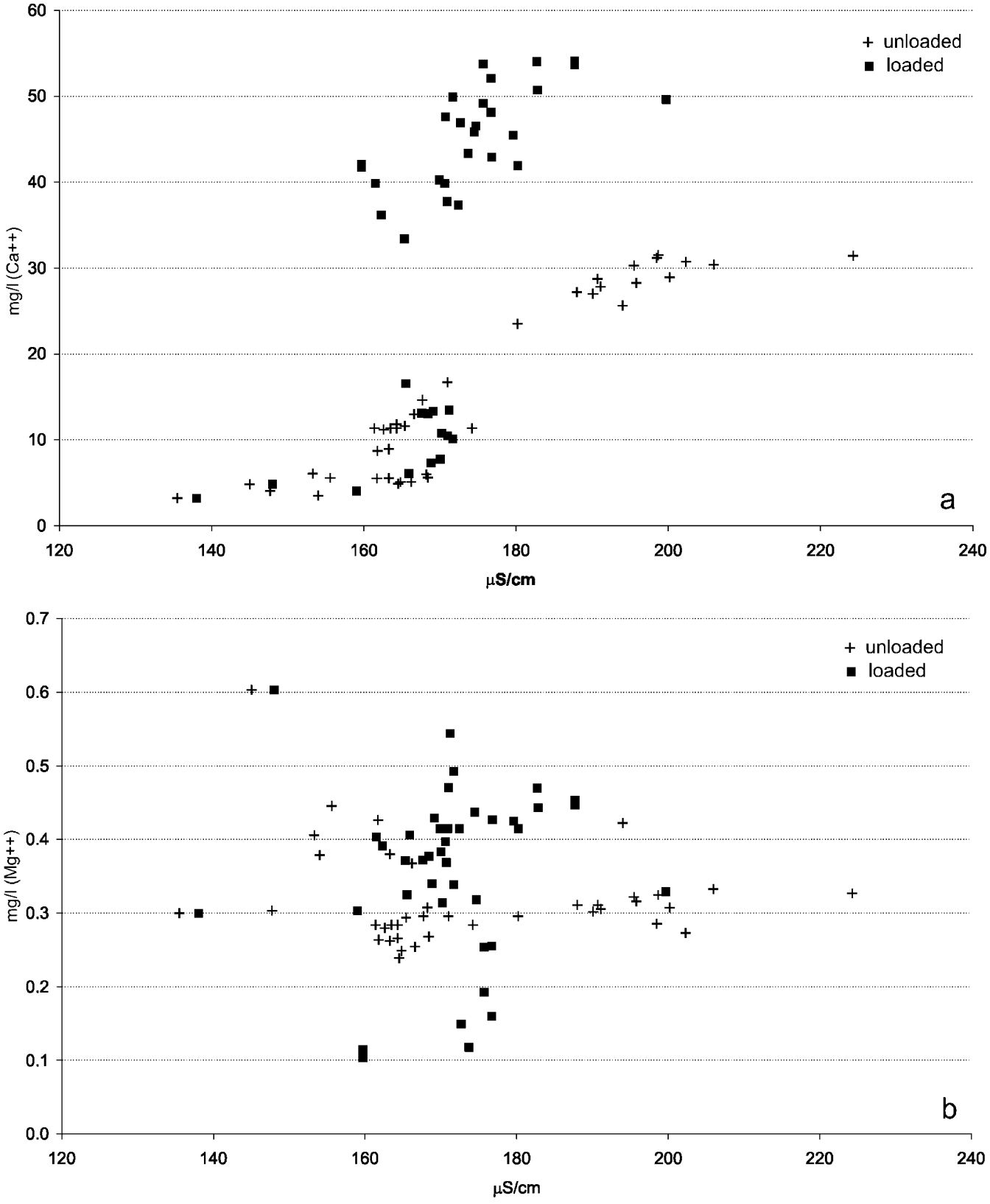

Fig. 9 **a** Ca^{++} concentration versus electrical conductivity and **b** Mg^{++} concentration versus electrical conductivity in circulation water throughout the experiment

 DOI 10.1007/s10040-006-0064-x

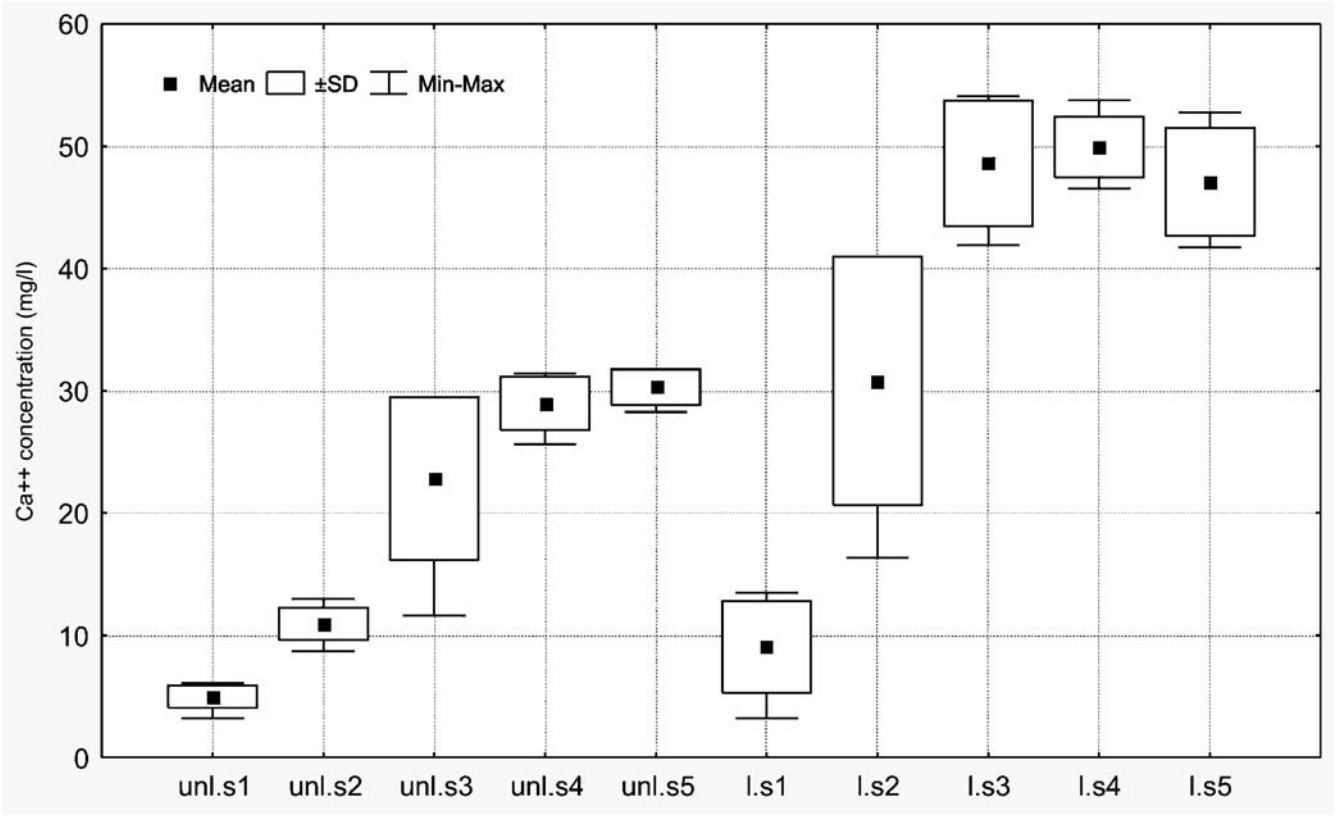

Fig. 10 Main statistical parameters (*SD* standard deviation) of Ca^{++} concentrations in the unloaded (*unl.*) and loaded (*l.*) block circuits, with reference to the five identified time stages (from *s1* to *s5*)

Stress-strain analysis via numerical modelling

Because the stress magnitudes in the two rock blocks could not be directly measured, due to the configuration of the experimental apparatus, a finite-difference numerical model, based on the FLAC 4.0 software code (ITASCA 2000), was implemented with the intention of indirectly evaluating the tensional state of the two blocks.

Two sections (transverse and longitudinal) of the rock block were analysed by using a square mesh (5 cm side) grid. The parameters for geomechanical characterization of the limestone were selected according to an elastic-perfectly plastic constitutive Mohr-Coulomb law. Their values (Table 3) were assigned on the basis of the results of laboratory tests on limestone samples collected from the same site as the one used for the physical analogue model (Martino et al. 2001). In particular, the geomechanical parameter values were assigned by using a statistical distribution without spatial control (Gaussian distributions with a variation coefficient of less than 30%, Martino et al. 2001). In the longitudinal section, account was taken of seepage through the rock mass holes. Since the model was two-dimensional, the simulation of groundwater flowpaths through the holes required the use of an "equivalent permeability" value; this value was set on the basis of an outflow of about 16 L/min, i.e. to the flow rate of the two pumps operating in the individual circuits. The simulation also took into account the possibility of groundwater circulating through the net of microcracks in the limestone. Based on the mapping of joints observable on the faces of the rock mass, the main discontinuities of the limestone, persisting through the entire simulated section, were replicated.

The results showed that the static load, applied during the experiment, induced tensile stresses in the rock mass of up to 20 kPa (Figs. 11 and 12). Furthermore, in the

Table 3 Geomechanical parameters used for numerical modelling: *den* density; *E* Young modulus; *K* bulk modulus; *G* shear modulus; *c* cohesion; ϕ angle of internal friction; *ten* tension cut off; *SD* standard deviation

	Den (kg/m^3)	SD (kg/m^3)	K (Pa)	SD (Pa)	G (Pa)	SD (Pa)	ϕ	SD (°)	c (Pa)	SD (Pa)	Ten (Pa)	SD (Pa)
Limestone	2,699	4.7	3.90E+09	7.80E+08	2.35E+09	4.73E+08	46	5.62	3.00E+07	5.87E+06	1.50E+07	2.94E+06
Joints	2,699	4.7	3.90E+09	7.80E+08	2.35E+09	4.73E+08	46	5.62	0.00E+00	0.00E+00	0.00E+00	0.00E+00

 DOI 10.1007/s10040-006-0064-x

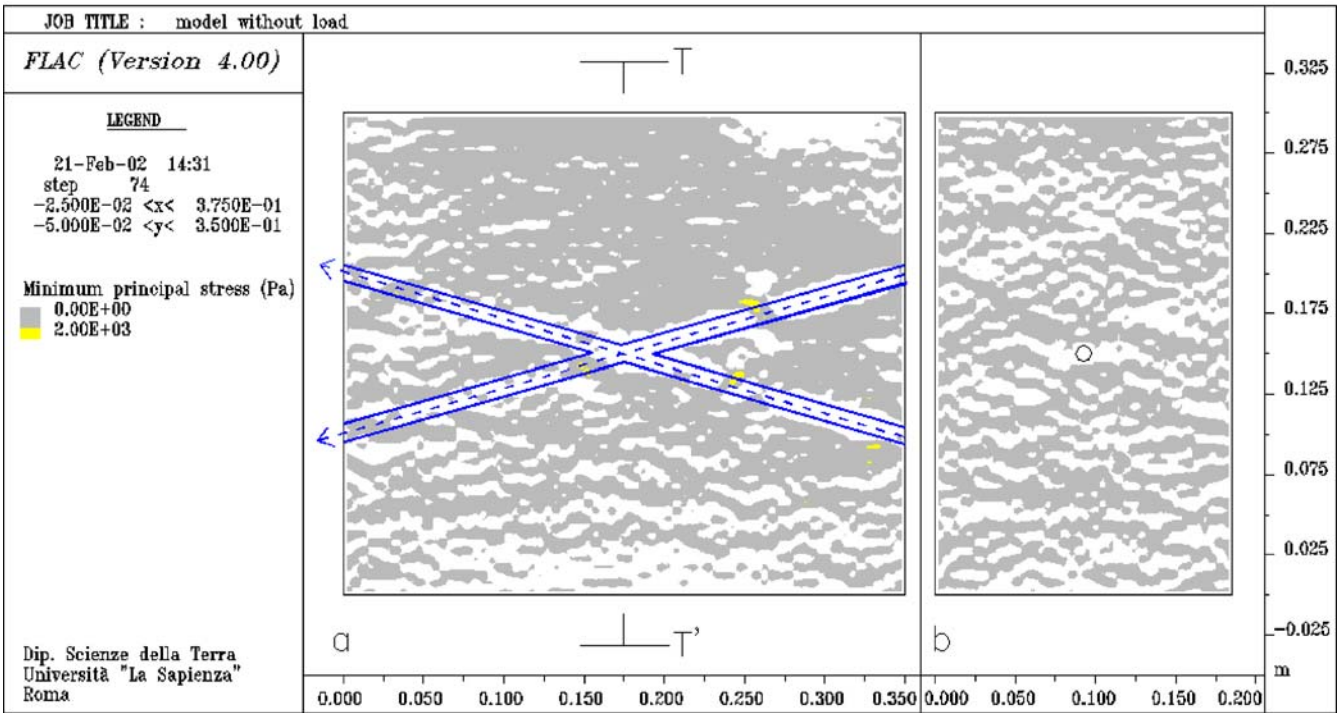

Fig. 11 Minimum principal stress distribution resulting from the numerical model for the unloaded block: **a** longitudinal block section; **b** transverse block section (along trace *TT'*); positive values *(Pa)* are in reference to tensile stress, *blue continuous lines* indicate the position of the holes within the block, *blue arrows* show flow direction. *White patches* indicate compressive stresses (negative values)

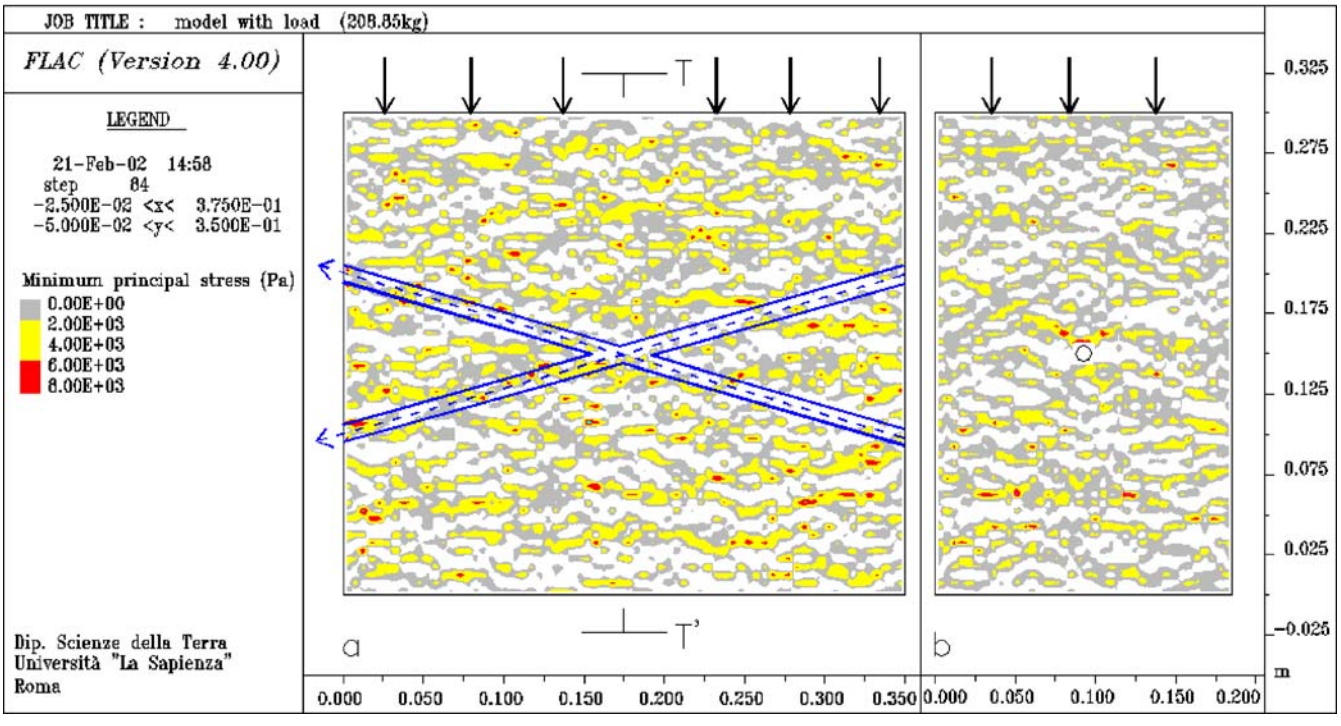

Fig. 12 Minimum principal stress distribution resulting from the numerical model for the block loaded with 208.85 kg: **a** longitudinal section, **b** transverse section (along trace *TT'*); positive values *(Pa)* are in reference to tensile stress, *blue continuous lines* indicate the position of the holes within the block, *blue arrows* show flow direction. *White patches* indicate compressive stresses (negative values)

 DOI 10.1007/s10040-006-0064-x

jointed longitudinal section, the distribution of tensile stresses matched the pattern of discontinuities inside the limestone (Fig. 13). In particular, tensile stresses mainly occurred close to the intersection between discontinuities. The holes in the rock mass appeared to play a role similar to the one of discontinuities. Indeed, under overload conditions, tensile stresses increased at intersections of both holes and joints. Numerical simulations under increased static load conditions (445.05 kg) showed a significant increase in tensional responses (Figs. 11 and 12); thus, the application of static loads during the experiment elicited areas of concentrated tensile stresses in the limestone. These areas appeared near flowpaths and/or at the points of intersection of persistent discontinuities in the rock blocks. These clusters of tensile stresses are likely to represent points of preferential dissolution by the turbulent flow of water in the rock blocks, as a result of combined chemical and mechanical action. This agrees with the results of physical–chemical monitoring, which indicate a significantly higher dissolution activity in the loaded mass circuit throughout the experiment.

Conclusions

Gravity-induced slope deformations in the carbonate central Apennines commonly occur near highly jointed rock masses hosting major karst aquifers; this fact suggests significant interactions between seepage, karst dissolution, tensional states and gravitational deformations. The case study discussed in this paper highlighted these interactions in the southern slope of the Peschiera Springs (Latium, Italy), i.e. the discharge area of one of the largest regional karst aquifers in Italy.

The development of a detailed geological-evolutionary model was the starting point for analysing the above interactions through an experimental approach, which relied on a physical analogue model, supported by numerical modelling of stress-strain conditions. The model was a physical replication of seepage inside the karst aquifer, under various tensional conditions in the limestone used for the experiment. The physical analogue model was based on an experimental apparatus consisting of two hydraulic circuits passing through each of two blocks of

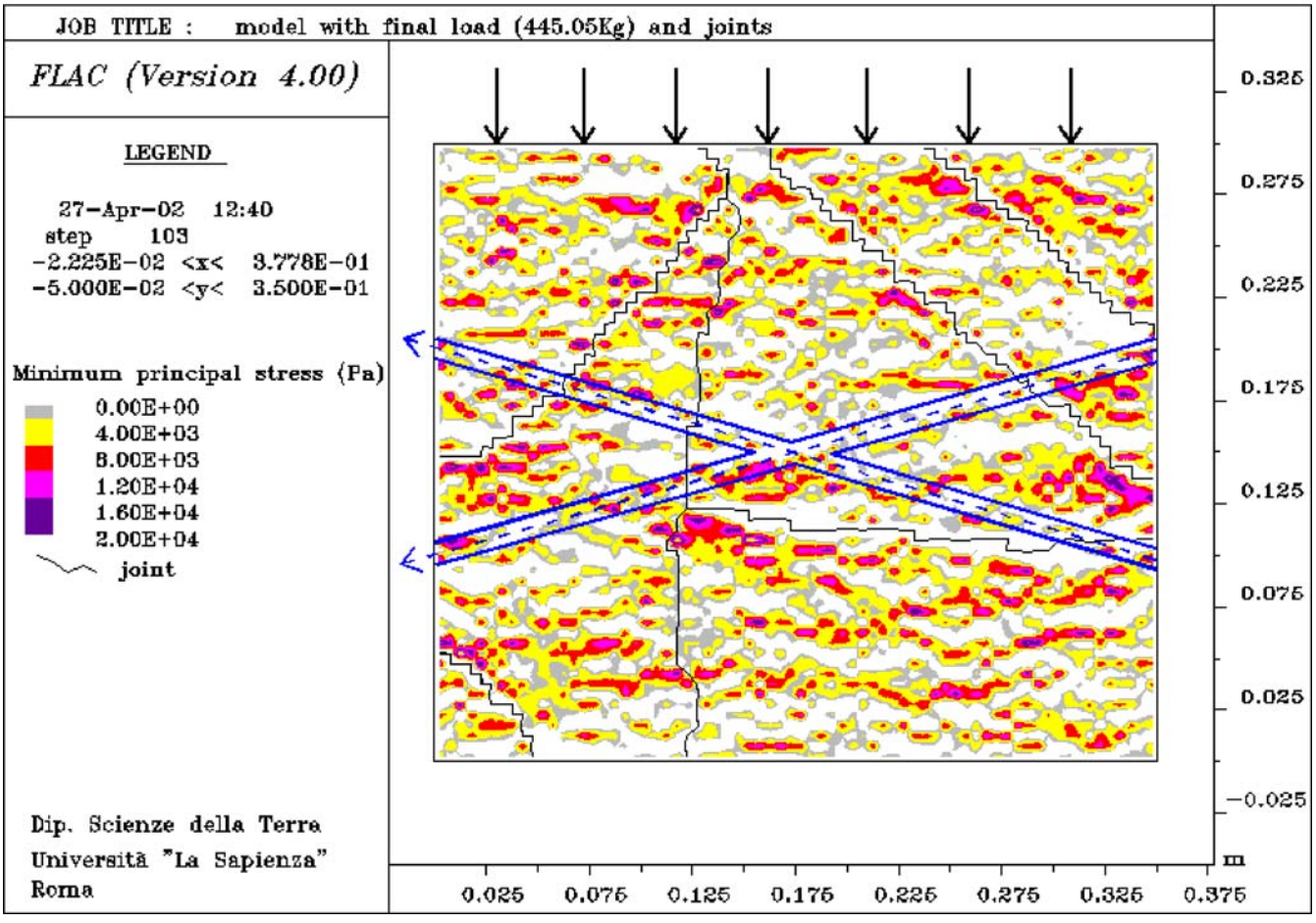

Fig. 13 Minimum principal stress distribution resulting from the numerical model for the block loaded with 445.05 kg (longitudinal section); positive values *(Pa)* are in reference to tensile stress, *blue continuous lines* indicate the position of the holes within the block, *blue arrows* show flow direction. *White patches* indicate compressive stresses (negative values)

 DOI 10.1007/s10040-006-0064-x

limestone collected from the slope; these circuits induced a turbulent flow at the crossing between two diagonal holes drilled in each block. During the experiment, one of the two blocks was subjected to a static load in order to elicit tensile stresses inside it. The physical and chemical monitoring data of the experiment demonstrated that dissolution, mainly of $CaCO_3$, was more pronounced in the loaded block circuit and that it was mainly controlled by temperature until the opening of microcracks was observed, as a consequence of load and dissolution interaction. The intercommunication between external saturation water and block circuit water, due to the opened microcracks in the loaded block, induced a dilution in the block circuit water as well as increasing water losses from the same circuit. This process was confirmed by the overload of the fractured block; the dilution in the overload block circuit increased after the application of a double load.

Numerical modelling made it possible to evaluate the tensional condition in the rock block as well as to establish correlations between evidence of jointing, elicited tensional states and seepage. The numerical model showed that, under the tensional conditions in which a higher dissolution activity was measured, tensile stresses tended to cluster along persistent joints, especially at their points of intersection or at their intersection with flowpaths. Hence, these clusters of tensile stresses may be regarded as points of preferential and accelerated dissolution. In the natural system, these points may be discontinuities in the rock mass, stress-relief bands and tensile stress clusters in the limestone underlying the aquifer, thereby causing the formation of karst caves. The results obtained in this experimental work also prove that the use of adequately integrated modelling approaches (such as physical analogue and numerical models) are key tools for validating and quantitatively integrating the reconstructed geological-evolutionary model based on field surveys.

Acknowledgements The authors are indebted to G. Scarascia Mugnozza for contributing to the fine-tuning of the engineering-geological model, to C. Romagnoli and G. Martino (ACEA S.p.A.) for providing technical documentation, to S. Tersigni (ISTAT) for revising the geochemical data, to I.D. Sasowsky (University of Akron, USA) for his revision of the paper. Comments by the editor and by the anonymous reviewers were highly appreciated. The study was funded by a research grant of the Italian Ministry of Education, Universities and Scientific Research (MIUR–COFIN2003), co-ordinator: A. Prestininzi.

References

Alberto W, Carraro F, Giardino M, Martinetti G, Sassone P, Tiranti D (2004) Segnalazioni di sinkholes a vari stadi di evoluzione nelle Alpi Occidentali (Individuation of sinkholes in different evolutive stages in the Western Alps). Proc. Workshop "Stato dell'arte sullo studio dei fenomeni di sinkholes e ruolo delle amministrazioni statali e locali nel governo del territorio", Rome, March 2004, pp 37–52

Alkattan M, Oelkers EH, Dandurand JL, Schott J (1998) An experimental study of calcite and limestone dissolution rates as a function of pH from −1 to 3 and temperature from 25 to 80°. Chem Geol 151:199–214

Bauer S, Liedl R, Sauter M (2003) Modeling of karst aquifer genesis: influence of exchange flow. Water Resour Res 39 (10):1285

Boni CF, Bono P, Capelli G (1986) Schema idrogeologico dell'Italia Centrale (Hydrogeological scheme of central Italy). Mem Soc Geol It 35:991–1012

Boni CF, Capelli G, Petitta M (1995) Carta idrogeologica dell'alta e media Valle del F. Velino (Hydrogeological map of the higher-middle Velino River Valley). System Cart, Rome

Boni CF, Beaubien SE, Ciotoli G, Di Filippo M, Lombardi S, Nolasco F, Petitta M, Toro B, (2004) Sinkhole hazard in Italy: research projects in the S. Vittorino Plain (central Italy). 32 International Geological Congress, Florence, August 2004, G02.04 (144)

Bray JW, Goodman RE (1976) Toppling of rock slopes. Proc. Special Conference on Rock Engineering for foundations and slopes, ASCE, Boulder, CO, August 1975, pp 201–234

Brunamonte F, Prestininzi A, Romagnoli C (1994) Geomorfologia e caratteri geotecnici dei depositi di terre rosse nelle aree carsiche degli Aurunci Orientali (Lazio Meridionale, Italia)-Geomorphological and geomechanical features of reddish soils in the eastern Aurunci karstic area (Latium, Italy). Geol Romana 30:465–478

Capelli G, Petitta M, Salvati R (2000) Relationships between catastrophic subsidence hazards and groundwater in the Velino Valley (central Italy). Proc. SISOLS 2000, Ravenna, Italy, September 2000, pp 123–135

Chemenda A, Bouissou S, Bachmann D (2005) Three-dimensional physical modelling of deep-seated landslides: new technique and first results. J Geophys Res 110:(F04004)8

Ciotoli G, Di Filippo M, Nisio S, Romagnoli C (2001) La Piana di S. Vittorino: dati preliminari sugli studi geologici, strutturali, geomorfologici, geofisici e geochimica (The S. Vittorino Plain: preliminary data on geological, structural, geomorphological, geophysical and geochemical studies. Mem Soc Geol It 56:297–308

Defrancesco F, Ziglio G, Zottele L, Bernardi F (1997) Cinetica di formazione delle acque minerali naturali: un modello di laboratorio per il suo studio (The kinetics of the genesis of natural mineral waters: a laboratory model). Riv Sci Aliment 26 (2):18–33

Dijk P, Berkovitz B (1998) Precipitation and dissolution of reactive solutes in fractures. Water Resour Res 34(3):457–470

Dreybrodt W (1981) Kinetics of dissolution of calcite and its application to karstification. Chem Geol 31:245–269

Dreybrodt W (1987) The kinetics of calcite dissolution and its consequences to karst evolution from the initial to the mature stage. Natl Speleol Soc Bull 49:31–49

Dreybrodt W (1988) Processes in karst systems. Springer series in physical environments, Springer, Berlin Heidelberg New York, p 288

Dreybrodt W (1990) The role of dissolution kinetics in the development of karstification in limestone: a model simulation of karst evolution. J Geol 98:639–655

Dreybrodt W (1991) Theoretical and experimental results on the kinetics of calcite dissolution and precipitation, World Karst Correlation, International Symposium on Karst of Inner Plate Region with Monsoon Climate, Guilin, China, July/August 1991, pp 17–31

Dreybrodt W (1996) Principle of early development of karst conduits under natural and man-made conditions revealed by mathematical analysis of numerical models. Water Resour Res 32(9):2923–2935

Dreybrodt W (1997) Limestone dissolution rates in karst environments. In: Sauter J (ed) Modelling in karst systems. Lang, Bern, pp 167–183

Faccenna C, Florindo F, Funiciello R, Lombardi S (1993) Tectonic setting and sinkholes features: case histories from western central Italy. Quat Proc 3:47–56

Griffith AA (1920) The phenomena of rupture and flow in solids. Phil Trans Roy Soc London A 221:163–198

Groves GC, Howard AD (1994) Early development of karst systems. 1. Preferential flow path enlargement under laminar flow. Water Resour Res 30(10):2837–2846

ITASCA (2000) FLAC 4.0: user manual. Itasca Consulting Group (licensee: DST–"La Sapienza", serial No. 213-039-0127-16143), Itasca Consulting Group, Rome

Kharaka YK, Gunter WD, Aggarwal PK, Perkins EH, DeBraal JD (1988) SOLMINEQ88: a computer program for geochemical modelling of water-rock interactions. Water Resources Inv. Report, 88–4227, US Geological Survey, Reston, VA

Lennart Sjoberg E, Richard DT (1984) Temperature dependence of calcite dissolution kinetics between 1 and 62°C at pH 2.7 to 8.4 in aqueous solutions. Geochim Cosmochim Acta 48:485–493

Liu Z, Dreybrodt W (1997) Dissolution kinetics of calcium carbonate minerals in H2O-CO2 solutions in turbulent flow: the role of the diffusion boundary layer and the slow reaction $H_2O + CO_2H^+ + HCO_3^-$. Geochim Cosmochim Acta 61:2879–2889

Maffei A, Martino S, Prestininzi A (2005) From the geological to the numerical model in the analysis of the gravity-induced slope deformations: an example from the Central Apennines (Italy). Eng Geol 78:215–236

Martino S, Prestininzi A, Scarascia Mugnozza G (2001) Deep-seated gravitational deformations: parameters from laboratory testing for analogical and numerical modelling. Rock mechanics, a challenge for society, EUROCK 2001, Espoo, Finland, Balkema, Lisse, pp 137–142

Martino S, Prestininzi A, Scarascia Mugnozza G (2004) Geological-evolutionary model of a gravity-induced slope deformation in the carbonate Central Apennines (Italy). Q J Eng Geol Hydrogeol 37:31–47

Middleton GV, Wilcock PR (1994) Mechanics in the earth and environmental sciences. Cambridge University Press, New York, pp 459

Mylroie JE, Carew JL (1995) Karst development on carbonate islands. In: Budd DA, Harris PM, Saller A (eds) Unconformities and porosity in carbonate strata. American Association of Petroleum Geologists. Memoir 3:55–76

Nolasco F (1998) La Piana di S. Vittorino. Contributo allo studio dei processi evolutivi dei rischi e della prevenzione (The S. Vittorino Plain: a contribution for the study of evolutionary processes, risks and prevention). Technical report for the convention Regione Lazio-ACEA SpA, Rome

Novak CF (1993) Modelling mineral dissolution and precipitation in dual-porosity fracture-matrix systems. J Contam Hydrol 13:91–115

Petitta M, Tallini M, Benedetti G, Del Monaco F (2003) Fracture pattern influence on groundwater discharge along the tectonic border of karst aquifers (Velino Valley, Central Italy). Proc. Hydrogeology in Fractured Rocks, Prague, September 2003, pp 85–86

Plummer LN, Wigley TML (1976) The dissolution of calcite in CO_2 saturated solutions at 25°C and 1 atmosphere total pressure. Geochim Cosmochim Acta 40:191–202

Plummer LN, Wigley TML, Parkhurst DL (1978) The kinetics of calcite dissolution in CO_2-water systems at 5–60°C and 0.0–1.0 atm CO_2. Amer J Sci 278:179–216

Pocar D (1996) Reazioni organiche: teorie e pratica (Organic reactions: theory and practise). Casa Editrice Ambrosiana, Milano

Polak A, Elsworth D, Liu J, Grader AS (2004) Spontaneous switching of permeability changes in a limestone fracture with net dissolution. Water Resour Res 40(W03502). DOI 10.1029/2003WR002717

Rege DS, Fogler HS (1989) Competition among flow, dissolution and precipitation in porous media. AIChE J 35(7):117–1185

Salvati R, Sasowsky ID (2002) Development of collapse sinkholes in areas of groundwater discharge. J Hydrol 264:1–11

Sanford WE, Konikow L (1989) Porosity development in coastal carbonate aquifers. Geology 17:249–252

Sasowsky ID, White WB (1994) The role of stress release fracturing in the development of cavernous porosity in carbonate aquifers. Water Resour Res 30(12):3523–3530

Savage WZ, Smith WK (1986) A model for the plastic flow of landslides. US Geol Surv Prof Pap 1385:1–32

Singurindy O, Berkowitz B (2003) Evolution of hydraulic conductivity by precipitation and dissolution in carbonate rock. Water Resour Res 39(1):1016

Teusch G, Sauter M (1991) Groundwater modelling in karst terranes: scale effects, data acquisition and field validation. Proc. Third Conference on Hydrogeology, Ecology, Monitoring and Management of Groundwater in Karst Terranes. Dec. 1991, Nashville, TN

Wittke W (1990) Rock mechanics: theory and applications with case histories. Springer, Berlin Heidelberg New York, 1075 p

Zischinsky U (1969) Uber Sackungen. Rock Mech 1:30–52